T* Integral Analyses of Shell Structures with Through-Wall Cracks for Nonlinear deformation Problems

T. Nishioka[1], T. Miyanishi[1], and T. Fujimoto[1]

Summary

In this study, in order to deal with arbitrary shell structures such as a thin plate and pipe, the finite element method using the degeneration shell element was used, and numerical simulations were performed about the nonlinear fracture problem for shell structures. The path-independence of $T_{,1}^*$ integration was derived based on the second Kirchhoff stress and Green-Lagrange strain to which the nonlinear term was added, and the evaluative formula of $T_{,1}^*$ integration along the crack front tip for shell structures was shown. Moreover, we explained aspects and differences in reaching the starting state of fracture depending on analysis conditions.

Introduction

Today, pipelines are built in ships, along the coast and at the bottom of ocean to transport oil and natural gas. Fracture of these ocean and coastal structures could cause accidents in which internal fluid flows to the outside, resulting in serious damage to the marine environment. This is because huge leaks arises when large-scale crack extension is caused by inner pressure triggering a pipe burst. In this fracture, it is already known that the crack tip snakes its way toward the axis of the pipe, and that these aspects are dependent on the crack speed and the shape of the pipe.[1] To prevent such environmental accidents, some research on the damage process and fracture mechanisms of pipe have been made.[2] However, sufficient results have not been reported about the prediction of the fracture aspects after the occurrence of the accident and the damage control adapting the predicting method. In this research, these problems with pipelines are analyzed by numerical simulation. The ultimate goal of this research is to evaluate fracture and crack extension behaviors with high precision. In order to deal with arbitrary shell structures, such as a thin plate, pipe shape, etc., the finite element method using the degeneration shell element [3][4] was formulized. The Newton-Raphson method was used for analysis technique of nonlinear problems, such as large deformation and elastic-plasticity. If crack length becomes large when a crack extends from inner pipe to its outer area, the steel plate near the crack will become deformed greatly. Therefore, it is necessary to develop effective criteria for nonlinear fracture problems of large deformation for shell structures. In this study, the analysis uses the second Kirchhoff stress and Green-Lagrange strain. In order to take into consideration the large deformation caused by the geometric nonlinear, the nonlinear term was added to Green-Lagrange strain. The path-independence of $T_{,1}^*$ integration was derived based on these stress and strain, and the evaluative formula of $T_{,1}^*$ integration along the crack front tip for shell structures was shown. In order to examine the validity of these formulizations,

[1] Simulation Engineering Laboratory, Department of Ocean Mechanical Engineering, Kobe University of Mercantile Marine, Higashinada-ku, Kobe, 658-0022, Japan

we calculated the normalized stress intensity factor in the plate bending problem, and compared with the result of Nishioka et al [5]. Furthermore, the numerical simulations for elastic infinitesimal and large deformation, elastic-plastic infinitesimal and large deformation were performed about A533B pipe structure with through wall crack, and the results were shown.

The finite element method using the degeneration shell element

The concept of shell element, a global, a local, a curvilinear and a nodal coordinate systems are shown in Fig.1. The displacement field in a degeneration shell element is defined by formula (1). The degrees of freedom consist of the three displacement components (u, v, w) and two independent rotation components (α, β).

$$\begin{Bmatrix} u \\ v \\ w \end{Bmatrix} = \sum_{i=1}^{n} N_i(\xi,\eta) \begin{Bmatrix} u_i \\ v_i \\ w_i \end{Bmatrix}_{mid} + \sum_{i=1}^{n} N_i(\xi,\eta)\zeta \frac{t_i}{2} \begin{bmatrix} P_{1i}^x & -P_{2i}^x \\ P_{1i}^y & -P_{2i}^y \\ P_{1i}^z & -P_{2i}^z \end{bmatrix} \begin{Bmatrix} \alpha_i \\ \beta_i \end{Bmatrix} \quad (1)$$

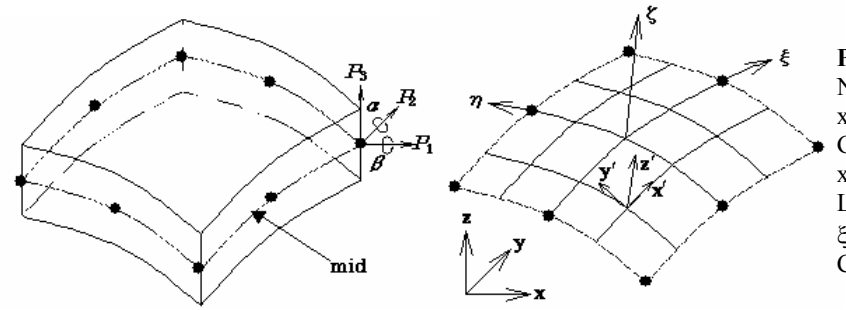

P_1, P_2, P_3 : Nodal-coordinate
x, y, z : Global-coordinate
x', y', z' : Local-coordinate
ξ, η, ζ : Curvilinear-coordinate

(a) Shell Element and Nodal Coordinates. (b) Global, Local and Curvilinear Coordinates.
Fig.1 Conceptual figure of 8-nodes shell element and coordinate systems

Where, (u, v, w) is the displacement component based on a global coordinate system, $N_i(\xi, \eta)$ is the element shape function based on a curvilinear coordinate system and t is the plate thickness. The subscript is the middle surface in an element. $\mathbf{P_1}$ and $\mathbf{P_2}$ are the nodal coordinate systems defined on each node, and (α, β) express the rotations of $\mathbf{P_1}$ and $\mathbf{P_2}$ axis. A local coordinate system defines x'-y' tangent plane to each integral point, and the z' axis expresses the normal direction of the x'-y' tangent plane. In order to establish a plane stress approximation (σ_{zz}=0), the stress and strain are defined on a local coordinate system. The tangential stiffness matrix for nonlinear problems, such as elastic-plastic and geometric nonlinear problem can be expressed by formula (2)

$$d\psi = [K]'_e dq = \int_{V_0} \mathbf{B'}^{\mathrm{T}} D' \mathbf{B'} dV_0 + \int_{V0} d\mathbf{B'}^{\mathrm{T}} \sigma' dV_0 \quad (2)$$

" ' " expresses the quantity defined by the local coordinate system. Elastic-plastic calculation is possible by replacing $\mathbf{D'}$ with $\mathbf{D'}_{ep}$ which is elastic-plastic stress-strain matrix. Mises's rule is used as the yield criterion. $\mathbf{B'}$ is the matrix which converts the displacement components defined by a global coordinate system to the strain of a local coordinate system on an integral point in an element. In order to take into consideration

the large deformation, Green-Lagrange is expressed as formula (3) (4) by using the Von-Karman assumption [6], which is that derivatives of u' and v' with respect to x', y' and z' are small and the variation of w with z is neglected. Therefore, **B'** becomes the form including the nonlinear term. $\mathbf{B_0}'$ is the same form as the infinitesimal deformation analysis, and $\mathbf{B_L}'$ is only dependent on displacement. Moreover, the Newton-Raphson method is used as the analysis technique of the nonlinear problem.

$$\begin{Bmatrix} \varepsilon_{x'x'} \\ \varepsilon_{y'y'} \\ \gamma_{x'y'} \\ \gamma_{z'x'} \\ \gamma_{z'y'} \end{Bmatrix} = \begin{Bmatrix} \dfrac{\partial u'}{\partial x'} \\ \dfrac{\partial v'}{\partial y'} \\ \dfrac{\partial u'}{\partial y'} + \dfrac{\partial v'}{\partial x'} \\ \dfrac{\partial w'}{\partial x'} + \dfrac{\partial u'}{\partial z'} \\ \dfrac{\partial w'}{\partial y'} + \dfrac{\partial v'}{\partial z'} \end{Bmatrix} + \begin{Bmatrix} \dfrac{1}{2}\left(\dfrac{\partial w'}{\partial x'}\right)^2 \\ \dfrac{1}{2}\left(\dfrac{\partial w'}{\partial y'}\right)^2 \\ \dfrac{\partial w'}{\partial x'} + \dfrac{\partial w'}{\partial y'} \\ 0 \\ 0 \end{Bmatrix} = \varepsilon_0' + \varepsilon_L' \quad (3)$$

$$\boldsymbol{\varepsilon}' = \mathbf{B}'\mathbf{u} = \left(\mathbf{B}_0 + \mathbf{B}_L\right)\mathbf{u} \quad (4)$$

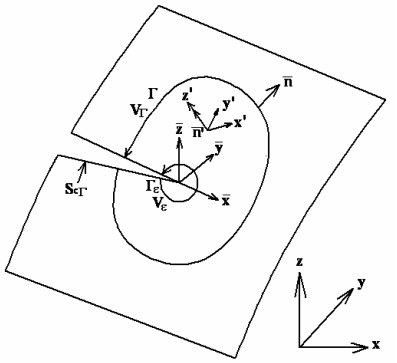

Fig.2 Definition of coordinate systems for crack problem

Fracture parameter $\Delta T_{,1}^*$

Expressing the fracture parameter $\Delta T_{,1}^*$ shown by Nishioka and Atluri et al [7][8], with the second Kirchhoff stress S_{ij} and Green-Lagrange strain λ_{ij}, formula (5) is obtained. In order to take into consideration the large deformation caused by geometric nonlinearity, Green-Lagrange strain can be expressed by the formula (3). Even if a nonlinear term is added to Green-Lagrange strain, path-independence of $\Delta T_{,1}^*$ is maintained. In static elastic fracture, $\Delta T_{,1}^*$ is equal to the static J of Rice [10] expressed by Caucy's stress and Almansi's strain.

$$\begin{aligned} \Delta T_{,1}^* &= \int_{\Gamma_\varepsilon}[\Delta_0 W n_1 - F_{ik}\left({}_0\tilde{t}_k + \Delta_0\tilde{t}_k\right)\Delta u_{i,1} - F_{ik}\Delta_0\tilde{t}_k u_{i,1}]dS_0 \\ &= \int_{\Gamma+S_{c\Gamma}}[\Delta_0 W n_1 - F_{ik}\left({}_0\tilde{t}_k + \Delta_0\tilde{t}_k\right)\Delta u_{i,1} - F_{ik}\Delta_0\tilde{t}_k u_{i,1}]dS_0 \\ &+ \int_{V_\Gamma - V_\varepsilon}\left[\left(\lambda_{ij,1} + \frac{1}{2}\Delta\lambda_{ij,1}\right)\Delta S_{ij} - \left(S_{ij,1} + \frac{1}{2}\Delta S_{ij,1}\right)\Delta\lambda_{ij}\right]dV_0 \end{aligned} \quad (5)$$

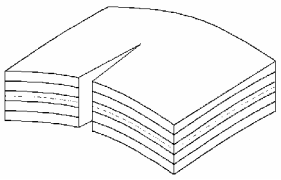

Fig.3 Crack front in shell structure

Where, a subscript "0" is the quantity defined by the initial coordinate, a subscript "Δ" is the incremental quantity, t_j is surface force, u_j is displacement, W is stress density $\Delta W=(S_{ij}+\Delta S_{ij}/2)\Delta\lambda_{ij}$, F_{ij} is deformation gradient tensor. In addition, all quantity $T_{,1}^*$ can be expressed by the following formula.

$$T_{,1}^* = \sum \Delta T_{,1}^* \quad (6)$$

Considering the possible case of arbitrary shell structures with a through wall crack a global coordinate (x, y, z), a local coordinate (x', y', z'), and a crack tip coordinate $(\bar{x}, \bar{y}, z)$ systems are shown in Fig.2. As shown in Fig.3, a shell element is divided into several layers across the thickness, and $\Delta T_{,1}^*$ is evaluated at the middle face of each layer.

Correcting $\Delta T_{,1}^{*}$ obtained by formula (5) to $\Delta T_{,1}^{*}$ along the crack front in the arbitrary evaluation layer, formula (7) is obtained. Such a fracture parameter J for shell structures is shown by Watanabe et al [9]. In the case of infinitesimal deformation, formula (7) agrees with Watanabe's J.

$$\Delta T_{,1}^{*} = \int_{\Gamma+S_{c\Gamma}} \left\{ \Delta_0 \overline{W} \overline{n}_1 - F_{ik}\left({}_0\overline{\overline{t}}_k + \Delta_0 \overline{\overline{t}}_k\right) \frac{\partial \Delta \overline{u}_i}{\partial \overline{x}_1} - F_{ik} \Delta_0 \overline{\overline{t}}_k \frac{\partial_0 \overline{u}_i}{\partial \overline{x}_1} \right\} dc$$
$$+ \int_A \left\{ \frac{\partial \Delta_0 \overline{W}}{\partial z'} \overline{n}_1' - \frac{\partial}{\partial z'} \left(F_{ik}\left({}_0\overline{\overline{t}}_k + \Delta_0 \overline{\overline{t}}_k\right) \frac{\partial \Delta \overline{u}_i}{\partial \overline{x}_1} \right) - \frac{\partial}{\partial z'} \left(F_{ik} \Delta_0 \overline{\overline{t}}_k \frac{\partial_0 \overline{u}_i}{\partial \overline{x}_1} \right) \right\} dA \qquad (7)$$
$$+ \int_{V_\Gamma - V_\varepsilon} \left[\left(\overline{\lambda}_{ij,1} + \frac{1}{2} \Delta \overline{\lambda}_{ij,1} \right) \Delta \overline{S}_{ij} - \left(\overline{S}_{ij,1} + \frac{1}{2} \Delta \overline{S}_{ij,1} \right) \Delta \overline{\lambda}_{ij} \right] dV_0$$

Where, a subscript "-" is the quantity defined by crack tip coordinate, n_i is normal vector for Γ, n_i is normal vector for A, Γ is line integral path, A is the area surrounded by Γ.

Results and discussions

Fig.4 shows the model in which the bending moment load is distributed at both ends of the plate. The material properties and the size used for calculation are shown on Table1, and the model was analyzed as an elastic infinitesimal deformation. The total nodal points are 1281 and elements are 400.

Fig.5 shows a comparison with respect to a/W of the normalized stress intensity factor F_1 obtained by this calculation and those of Nishioka [5] and Watanabe [9]. F_1 is calculated by formula (8) and the value calculated on the surface of plane thickness (ζ=±1.0) is used as the $T_{,1}^{*}$ value.

$$F_1 = K_1 \Big/ \sigma\sqrt{\pi a} \qquad (8)$$

Where $K_1=(\kappa T_{,1}^{*})^{1/2}$ is stress intensity factor, κ=E at a plane stress and elastic problem, σ_0 is bending stress.

When the normalized stress intensity factor F_1 with respect to a/W in Fig.5 is compared with Nishioka's result, F_1 obtained in this study is lower than Nishioka's result. However, Watanabe calculates by the same method as this study, so it is well in agreement with Watanabe's result. On the other hand, Nishioka calculates by the combined method of FEM and analysis solution of the plate bending theory

Table. 1 Material properties

Young's modulus	E=206(GPa)
Poisson's rate	ν=0.3
Crack length	a=0.04(m)
Thickness	T=0.02(m)
Bending load	M=1961.33(Nm/m)

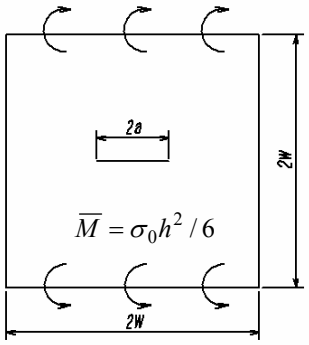

Fig.4 Numerical model for plate bending

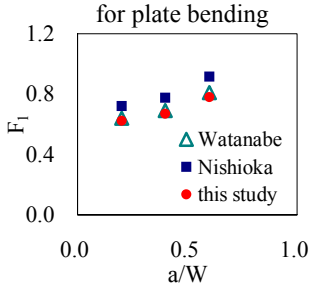

Fig.5 Comparisons of normalized stress intensity factor F_1

which takes shear deformation into consideration, so a more accurate result has been obtained than the one in this study.

Next, Fig.6 shows a cylindrical model with a through wall crack over which inner pressure is distributed. Assuming the material is A553B, the material properties and the size used for calculation are shown on Table 2. The work hardening at the time of elastic-plastic deformation can be obtained by formula (9).

$$\overline{\sigma} = \sigma_{YS} + n\overline{\varepsilon}_p \tag{9}$$

Table. 2 Material properties (A533)

Young's modulus	E=206(GPa)
Poisson's rate	ν=0.3
Crack length	a=0.05(m)
Thickness	T=0.001(m)
Radius	R=0.05(m)
Length	L=0.1(m)
Yield stress	σ_{ys}=550(MPa)
Harding rate	n=500(MPa)
Fracture toughness	T_c^*=98(kN/m)[11]

Fig.7 shows the mesh figure and integration paths of $T_{,1}^*$. The total nodal points are 2273 and elements are 720. We analyze this model for elastic infinitesimal deformation, elastic large deformation, elastic-plastic infinitesimal deformation, and elastic-plastic large deformation, and we show each result.

Fig.8 shows path-independence for elastic and elastic-plastic large deformations. The path-independence of $T_{,1}^*$ observed in elastic large deformation is less than 1%, so its independence is considered to be good. Since the path-independence is less than 5%, even taking the material nonlinear case into consideration, its independence can be considered to be good. Therefore, it can be said that evaluative formula of $T_{,1}^*$ expressed with the second Kirchhoff stress and Green-Lagrange's strain in this study is very effective for shell structures with through wall crack.

Fig.9 shows the change of $T_{,1}^*$ with incremental inner pressure. T_c^* in Fig.9 is the fracture toughness value of A533B. When large deformation is introduced in elastic and elastic-plastic problems, the load reaching T_c^* for large deformation is very large compared with infinitesimal deformation. This is probably because incremental stiffness becomes higher to take into consideration geometric nonlinearity, and much more load is needed for $T_{,1}^*$ to reach T_c^*. Moreover, when we compare elastic and elastic-plastic deformation, elastic-plastic deformation reaches the starting state of crack extension earlier. This is probably because we analyzed by load control, and large deformation occurred against the same load, allowing incremental degree of $T_{,1}^*$ to be bigger.

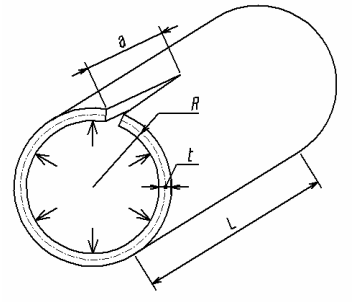

Fig. 6 Cylinder's model

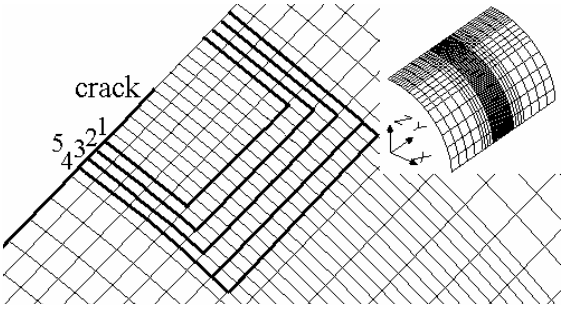

Fig.7 Mesh figure and integration path

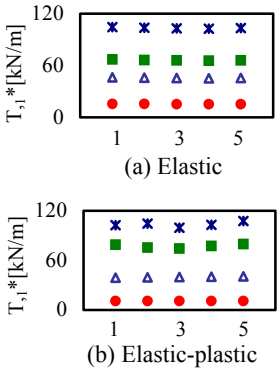

Fig.8 Path-independence of $T_{,1}^*$ for large deformation

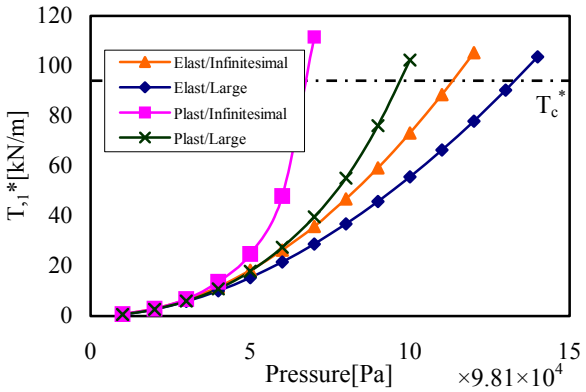

Fig.9 Change of $T_{,1}^*$ for incremental inner pressure

Conclusions

In this study, we reached the following conclusions.

(1) To address the shell structure crack problem, we showed fracture parameter T_c^* expressed with the second Kirchhoff stress and Green-Lagrange's strain considering geometric nonlinear.

(2) We performed elastic-plastic large deformation fracture analysis for arbitrary shell structures by using the degeneration shell element.

(3) We obtained good path-independence regardless of elastic, elastic-plastic, infinitesimal and large deformation. Therefore, evaluative formula of $T_{,1}^*$ shown in this study is very effective for fracture evaluation of shell structures.

(4) We explained aspects and differences in reaching the starting state of fracture of a cylinder structure.

References

1. Fujimoto K., Kakiuchi T. Shioya T. (2001): "Fundamental Study on Crack Propagation (On Cracks in Internally Pressurized Glass Tubes)", *Proceedings of the 2001 Annual Meeting of the JSME/MMD*, **1-16**, 467-468.
2. Kobayashi A. S. (1988): "Subsize Experiments and Numerical Modeling of Axial Rupture of Gas Transmission Lines", *Journal of Pressure Vessel Technology (ASME)*, **110**, 155-160.
3. Kawamata S. (1974): "Analysis of shell structures", *BAIFUKAN CO. LTD*, 84-116.
4. Ahmad S., Irons B.M., Zienkiewicz O.C. (1920): "Analysis of thick and thin shell structures by curved finite elements", *Int. J. Num. Meth. Engng*, **2**, 491-451.
5. Yagawa G. Nishioka T. (1979): "Finite Element Analysis of Stress Intensity Factors for Plane Extension and Plate Bending Problems", *Int. J. Num. Meth. Engng*, **14**, No.5, 727-740.
6. E. Hinton D. R. J. Owen. (1984): "Finite element Software for Plates and Shells", Pineridge Press LTD, 235-273.
7. Atluri S.N., Nishioka T., Nakagaki M. (1984): "Incremental Path-Independent Integrals in Inelastic and Dynamic Fracture Mechanics", *Eng. Fract. Mech.*, **20**, 2, 209-244.
8. Atluri. S.N., Kobayashi. A. S. (1986): "COMPUTATIONAL METHODS IN THE MECHANICS OF FRACTURE", *North-Holland*, **2**, 55-83.
9. Watanabe T. Yagawa G. (1983): "J-Integral Analyses of Plate and Shell Structures with Through-Wall Cracks using Thick Shell Element", *Transactions of JSME (Japanese)*, **49**(447), 1420-1426.
10. Rice J.R (1968): "A Path Independent Integral and the Approximate Analysis of Strain Concentration by Notches and Cracks", *J. Appl. Mech. (ASME)*, **35**, 379-386.
11. EPI Subcommittee. (1991): "Study on Elastic-Plastic Fracture Mechanics in Inhomogeneous Materials and Structures □", Nuclear Engineering Research Committee, *The Japan Welding Engineering Society*.